AIAA JOURNAL
Vol. 40, No. 10, October 2002

Shaping Optimal Design of Elastic Planar Frames with Frequency Constraints

D. Dinevski,* M. M. Oblak,† and M. Kegl‡
University of Maribor, 2000 Maribor, Slovenia

An approach to shaping optimal design of planar frames subject to eigenfrequency constraints, displacement constraints, and stress constraints simultaneously is described. The eigenfrequency constraints may be imposed at the deformed (due to the static load) configuration of the structure. For the shape representation of the structure, a design element technique is used. A frame structure is treated as assembled from several design elements, each of them being defined as a Bézier curve. The design variables may influence the position and the shape of each design element, plus the cross-sectional properties of beam elements. The optimal design problem is defined in a general form, and its solution, by employing gradient-based methods of mathematical programming, is discussed briefly. The structural response analysis is based on a nonlinear model that can handle virtually arbitrary large structural displacements. Two numerical examples illustrate the theory.

Nomenclature

A_i = area of the cross section
A_{xi} = shear area of the cross section
$\boldsymbol{b}$ = vector of design variables
C_i = centroid curve
E = elastic modulus of the material
$\boldsymbol{F}$ = vector of internal forces
f_i = eigenfrequencies
G = shear modulus of the material
h_i = constrained quantitites
I_i = moment of inertia of the cross section
$\boldsymbol{K}$ = stiffness matrix
$\boldsymbol{M}$ = mass matrix
P_i = Lagrange interpolation polynomial
p = external distributed force per unit length
$\boldsymbol{q}_i$ = position vector of a control point
$\boldsymbol{R}$ = vector of external forces
$\boldsymbol{r}_i$ = position vector
$\boldsymbol{u}$ = vector of structural displacements
$\boldsymbol{v}$ = vector of structural response variables
w = external distributed force per unit length
γ = shear strain
ε = extensional strain
λ_i = eigenvalues
φ = angle of inclination at the undeformed configuration
$\boldsymbol{\varphi}_i$ = eigenvector
ϕ = angle of rotation

I. Introduction

IN the past decade, the development of modern technologies and computer-aided manufacturing emphasized the significance of shape optimal design. An attractive foundation for general shape design procedures is offered by modern numerical methods such as the finite element method. Theoretically, there seem to be no difficulties because the finite element method is a common and general tool for structural analysis and because the structural shape can be quite arbitrarily described by adequate finite elements and nodal layout. However, this is surely incorrect because the introduction of shape optimal design sets some special requirements for finite elements. Generally, a finite element should not be sensitive to distortion of its undeformed shape. If this is not the case, difficulties emerge, and to maintain the integrity of the finite element mesh throughout the design process, an automatic mesh generator must be resorted to frequently during the shape optimal design process.

In recent years much research has been done in the development of beam finite elements. The main source of difficulties encountered by the researchers seems to be a consequence of the general syndrome, the field inconsistency[1] of the discretized strain fields. This leads to phenomena such as poor convergence, spurious strains/stresses, and several different kinds of locking. In an optimal design procedure, therefore, it is advantageous to employ a field-consistent element, for example, the beam element family proposed by Saje.[2,3] These elements do not suffer from any kind of locking, and the order of integration can be arbitrarily adjusted to assure the desired accuracy. Moreover, the efficiency and accuracy of these elements are excellent.

Much has been published concerning the field of optimal design of frame structures. Most of these publications deal with optimal design problems where only the sizing parameters, such as the areas of the cross section of individual frame members, are employed as design variables.[4–9] Shape optimal design problems are less frequently addressed. The field of shape optimization comprises several various classes of problems including variable cross-sectional properties along frame members, variable initial curvature of frame members, variable position of nodes including the supported ones, variable support conditions, and variable topology of the structure. Authors often address these problems separately, which results in special-purpose procedures applicable only in particular cases. For example, in Ref. 10, the problem of variable nodal positions of natural frequency-constrained frames is considered; in Ref. 11, stability and vibration-constrained frames and beams with variable position and stiffness of elastic hinges are discussed; in Ref. 12, topological optimization of skeletal structures is addressed; in Ref. 13, lateral buckling-constrained beams with variable support locations are discussed; and in Ref. 14, compliance-constrained beams with variable location of an additional support is considered. Although, in some papers, for example, Ref. 15, some of the problem classes are addressed simultaneously, there are, to the authors' knowledge, no papers except Ref. 16 addressing simultaneously variable cross-sectional properties, variable initial curvature of frame members, and variable position of supported and free nodes of frame structures that are allowed to undergo large nodal displacements and rotations.

In the present paper, the efficiency of the approach described in Ref. 16 is extended to the domain of dynamics in the sense that additional frequency constraints can be imposed to the structure. Note

Received 17 April 1999; presented as Paper 99-1392 at the AIAA/ASME/ASCE/AHS/ASC 40th Structures, Structural Dynamics, and Materials Conference, St. Louis, MO, 22–25 April 1999; revision received 25 April 2000; accepted for publication 13 May 2002.

*Postdoctoral Research Fellow, Faculty of Mechanical Engineering, Smetanova 17; dejan.dinevski@uni-mb.si. Member AIAA.
†Professor, Faculty of Mechanical Engineering, Smetanova 17.
‡Assistant Professor, Faculty of Mechanical Engineering, Smetanova 17.

that the solutions presented here enable dealing with frequency-constrained optimization of deformed (statically loaded) structures.

The design problem is defined in a form of a nonlinear problem of mathematical programming. The usual iterative solution technique is used by employing our own optimizer.[17,18]

II. Design Problem Formulation

Let the vector $\boldsymbol{b} \in R^{N_b}$ assemble N_b design variables, each of them representing an independent parameter that may be varied to alter the shape of the structure. The shape optimal design problem may, in this case, be formulated in the form of a nonlinear problem P of mathematical programming:

$$\min h_0, \qquad h_i \leq 0, \qquad 1 \leq i \leq N_h \tag{1}$$

where N_h is the number of imposed constraints. The objective function value $h_0 = h_0(\boldsymbol{b}, \boldsymbol{v})$ is often defined as the volume of the structure, whereas the constrained quantities $h_i = h_i(\boldsymbol{b}, \boldsymbol{v})$ usually concern the nodal displacements and rotations, element strains, natural frequencies, design variable limits, technological limitations, and so on. The symbol $\boldsymbol{v} \in R^{N_v}$ is the vector of structural response variables (where the frame structure is assumed to be discretized by the finite element method) and N_v is their number. In the present case, the vector of response variables is $\boldsymbol{v} = [\boldsymbol{u}^s, \lambda_1, \ldots, \lambda_{N_u}]^T$, where $\boldsymbol{u}^s \in R^{N_u}$ is the vector of structural displacements and $\lambda_1, \ldots, \lambda_{N_u}$ are the eigenvalues related to the structural eigenfrequencies $f_i, \ldots, f_{N_u}$ by $2\pi f_i = +\sqrt{\lambda_i}$.

In problem P, the design variables have to be considered as independent variables and the response variables as the dependent ones. The dependence of $\boldsymbol{v}$ on $\boldsymbol{b}$ is given implicitly by two equations. The first is the static structural response (equilibrium) equation

$$\boldsymbol{F}^s - \boldsymbol{R}^s = 0 \tag{2}$$

where $\boldsymbol{F}^s = \boldsymbol{F}^s(\boldsymbol{b}, \boldsymbol{u}^s) \in R^{N_u}$ and $\boldsymbol{R}^s = \boldsymbol{R}^s(\boldsymbol{b}, \boldsymbol{u}^s) \in R^{N_u}$ are the vectors of internal and external forces, respectively. Here, it will be assumed that externally applied loads are constant and of the fixed type and that the supports are not elastic. Therefore, the vector of external forces does not depend on $\boldsymbol{v}$ so that $\boldsymbol{R}^s = \boldsymbol{R}^s(\boldsymbol{b}) \in R^{N_u}$. The static case with elastic and skew-sliding supports is covered in Ref. 19.

The second equation is given by the usual eigenvalue problem

$$\left[\boldsymbol{K}^s - \lambda_j \boldsymbol{M}^s\right]\boldsymbol{\varphi}_j = 0 \tag{3}$$

where $\boldsymbol{K}^s = \boldsymbol{K}^s(\boldsymbol{b}, \boldsymbol{u}^s)$ is the tangential stiffness matrix, $\boldsymbol{M}^s = \boldsymbol{M}^s(\boldsymbol{b})$ is the mass matrix, λ_j is the jth eigenvalue, and $\boldsymbol{\varphi}_j$ is the corresponding eigenvector.

When it is assumed that all design variables are continuous, the problem P can usually be most efficiently solved by employing gradient-based methods of mathematical programming, for example, recursive quadratic programming or approximation methods. Commonly, the procedure is as follows[16]: The solution $\boldsymbol{b}^*$ of P is obtained as a limit of a sequence of approximate solutions $\{\boldsymbol{b}^{(i)}\}$, $i = 1, 2, 3, \ldots$. By this approach, $\boldsymbol{b}^{(0)}$ has to be chosen, whereas $\boldsymbol{b}^{(i+1)}$ is the solution of $P^{(i)}$ representing some approximation of P at the point $\boldsymbol{b}^{(i)}$.

The task of building up and solving $P^{(i)}$ is commonly done by the optimizer. To do this, the optimizer needs to be supplied with h_i and $\mathrm{d}h_i/\mathrm{d}\boldsymbol{b}$, $0 \leq i \leq N_f$, calculated at $\boldsymbol{b}^{(i)}$. Usually, this can be easily done once $\boldsymbol{v}$ and $\mathrm{d}\boldsymbol{v}/\mathrm{d}\boldsymbol{b}$ are calculated at $\boldsymbol{b}^{(i)}$. The vector $\boldsymbol{v}$ at $\boldsymbol{b}^{(i)}$ is calculated from the response equations given earlier, whereas $\mathrm{d}\boldsymbol{v}/\mathrm{d}\boldsymbol{b}$ at $\boldsymbol{b}^{(i)}$ can be calculated from the sensitivity equations presented in the design sensitivity section.

III. Shape Representation of a Frame Structure

To parameterize the shape of the structure, the design element technique[16] is employed. In this way, the number of design variables is kept at minimum, and the structural integrity can be fulfilled automatically throughout the iterative design process.

A design element may in general consist of any number of finite elements, and it may represent a whole structure or any part of it. The shape of each design element is defined by a planar Bézier curve, and the coordinates of the control points may be taken as design variables.

Combining the described approach with the beam element proposed in Refs. 2, 3, and 16, the shape of the jth beam belonging to the ith design element is completely specified by

$$\boldsymbol{r}_i = \boldsymbol{r}_i(\boldsymbol{b}, t), \qquad c_i^{j-1} \leq t \leq c_i^j$$
$$A_i = A_i(\boldsymbol{b}), \qquad A_{si} = A_{si}(\boldsymbol{b}), \qquad I_i = I_i(\boldsymbol{b}) \tag{4}$$

where $\boldsymbol{r}_i \in R^2$ is the position vector of a generic point lying on the centroid curve of the beam and A_i, A_{si}, and I_i are the area, the shear area, and the moment of inertia of the cross section, respectively. The cross-sectional quantities are assumed to be constant along the beam. The real parameters $c_i^{j-1} = \hat{c}_i^{j-1}(\boldsymbol{b})$ and $c_i^j = \hat{c}_i^j(\boldsymbol{b})$ determine the position and the length of the centroid curve of the beam and $t \in [0, 1]$.

To simplify the final equations, an independent variable s is introduced.[19] The variable $s \in [0, 1]$ determines the position along the centroid curve of the element, which makes the (previously independent) parameter t a dependent parameter by

$$t = \left(c_i^j - c_i^{j-1}\right)s + c_i^{j-1} \tag{5}$$

When this relationship is taken into account, the shape of the centroid curve of the jth beam finite element belonging to the ith design element is given as

$$\boldsymbol{r}_i^j = \boldsymbol{r}_i^j(\boldsymbol{b}, s), \qquad 0 \leq s \leq 1 \tag{6}$$

Let us focus on the definition of $\boldsymbol{r}_i$. In most practical applications, it is advantageous if we have direct control over the positions of both endpoints of the centroid curve C_i of the ith design element. Direct control means that the shape of C_i can be varied independently of the positions of these two points. This requirement can be fulfilled by expressing $\boldsymbol{r}_i$ in terms of a finite number of control points[20] including both endpoints and by employing appropriate blending functions.[20]

Let $\boldsymbol{q}_i^j \in R^2$, $1 \leq j \leq M_i$, be the position vector of a control point influencing the position and the shape of C_i. Now we need appropriate blending functions such that the curve C_i will start at $\boldsymbol{q}_i^1$ and end at $\boldsymbol{q}_i^{M_i}$. Additionally, C_i should follow approximately and without excessive oscillations the defining polygon[20] with $M_i - 1$ spans determined by the control points. Blending functions that fulfill all of these requirements are the Bézier blending polynomials (see Ref. 20).

Figure 1 is an example of a defining polygon determined by four control points and a corresponding Bézier curve, as well as a curve obtained by employing Lagrange interpolation polynomials as blending functions. The curve obtained by employing Lagrange interpolation polynomials benefits from that it passes through all control points. However, it oscillates too much. In the context of shape optimal design, this would cause an unstable and annoying design process with questionable results.

Based on the preceding discussion, let $\boldsymbol{r}_i$ be given by

$$\boldsymbol{r}_i = \sum_{j=1}^{M_i} B_{M_i,j}(t)\boldsymbol{q}_i^j \tag{7}$$

where $B_{M_i,j}$ is a Bézier blending polynomial. When all or some of the components of $\boldsymbol{q}^j$ $(1 \leq j \leq M)$ are taken as the design variables, so that

$$\boldsymbol{q}^j = \boldsymbol{q}^j(\boldsymbol{b}) \tag{8}$$

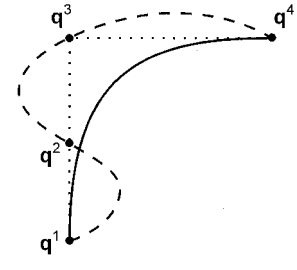

Fig. 1 Lagrange and Bézier polynomials employed as blending functions: ····, defining polygon; ——, Bézier; and – – –, Lagrange.

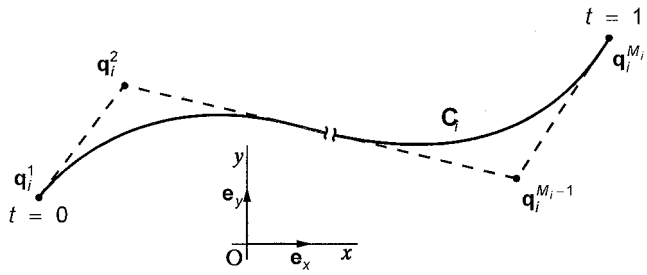

Fig. 2 Shape representation of C_i.

definition (4) offers large flexibility in controlling the position and the shape of C_i (Fig. 2). Note that more or less flexibility of C_i can be assured by simply increasing or decreasing the number of control points. In doing so, we do not need to worry about whether the shape of the curve in the engineering sense will remain realistic throughout the design process. The curve will never exhibit excessive oscillations, and it will always be contained within the convex hull[20] of the defining polygon, the largest convex polygon obtainable with the defining polygon vertices.

IV. Static Response Analysis

Static analysis is performed by solving the equilibrium equation (2). The usual iterative Newton method is employed, which means that in each iteration one has to calculate $\boldsymbol{F}^s$ and $\partial \boldsymbol{F}^s/\partial \boldsymbol{u}^s$. The vector $\boldsymbol{F}^s$ and the matrix $\partial \boldsymbol{F}^s/\partial \boldsymbol{u}^s$ are assembled from the corresponding element vectors and matrices.

For the reasons discussed in detail in Ref. 16, the highly accurate and initially curved beam finite element proposed by Saje[2,3] is selected in this work, and its governing equations are slightly modified[16] to fit nicely into the presented shape representation concept.

The beam finite element under consideration has $L = L(\boldsymbol{b})$ nodes, and its response is completely described by the following $n = m + 6$ scalar variables: four nodal displacements $u_1, \ldots, u_4$ of both end nodes, m nodal rotations $u_5, \ldots, u_{m+4}$, and two Lagrange multipliers (Refs. 2 and 3) u_{n-1} and u_n. For clarity, let the displacements and rotations of both end nodes be termed the external degrees of freedom (DOF). All other response variables are considered as element internal DOF. Let the element response variables be the components of the vector $\boldsymbol{u} = \boldsymbol{u}(\boldsymbol{b}) \in R^n$.

The rotation field is approximated by employing polynomial interpolation so that the angle of rotation $\phi = \phi(\boldsymbol{u}, s) \in R$ at an arbitrary point is expressed as

$$\phi = \sum_{i=1}^{m} P_i u_{i+4} \tag{9}$$

where $P_i = P_i(s)$ and P_i is the Lagrange interpolation polynomial.

The total angle of inclination of the normal to the cross section, measured with respect to the base vector $\boldsymbol{e}_x$, can in that case be expressed as $\varphi = \varphi_0 + \phi$, where φ_0 is the angle of inclination at the undeformed configuration. This angle is given by

$$\varphi_0 = \measuredangle(\hat{\boldsymbol{r}}'(\boldsymbol{b}, s), \boldsymbol{e}_x) \tag{10}$$

where the prime denotes differentiation with respect to s. It follows that $\varphi = \varphi(\boldsymbol{b}, \boldsymbol{u}, s)$.

The extensional strain $\varepsilon = (\boldsymbol{b}, \boldsymbol{u}, s) \in R$ of the centroid axis and the shear strain $\gamma = \gamma(\boldsymbol{b}, \boldsymbol{u}, s) \in R$ along the element are given by

$$\varepsilon = \frac{\zeta_1 \cos\varphi - \zeta_2 \sin\varphi}{AE}, \qquad \gamma = \frac{-\zeta_1 \sin\varphi - \zeta_2 \cos\varphi}{A_s G} \tag{11}$$

where E and G are the elastic and shear modulus of the material, respectively. The quantities $\zeta_1 \in R$ and $\zeta_2 \in R$ are expressed as

$$\zeta_1 = u_{n-1} - \int_0^s p_x(\boldsymbol{b}, q)\|\boldsymbol{r}'(\boldsymbol{b}, q)\|\,\mathrm{d}q$$

$$\zeta_2 = u_n + \int_0^s p_y(\boldsymbol{b}, q)\|\boldsymbol{r}'(\boldsymbol{b}, q)\|\,\mathrm{d}q \tag{12}$$

where the quantities $p_x = p_x(\boldsymbol{b}, s)$ and $p_y = p_y(\boldsymbol{b}, s)$ represent external distributed forces per unit length of the centroid curve.

The element internal forces $F_1, \ldots, F_n$ can now be written as

$$F_1 = -u_{n-1}, \qquad F_2 = u_n, \qquad F_3 = u_{n-1} - \int_0^1 p_x w\,\mathrm{d}s$$

$$F_4 = -u_n - \int_0^1 p_y w\,\mathrm{d}s \tag{13}$$

$$F_{i+4} = \int_0^1 \left\{EI\frac{\phi' P_i'}{w}\right\}\mathrm{d}s + \int_0^1 [AE\gamma\varepsilon - A_s G\gamma(1+\varepsilon) - p_z]w P_i\,\mathrm{d}s \qquad 1 \le i \le m \tag{14}$$

$$F_{n-1} = -\int_0^1 [(1+\varepsilon)\cos\varphi - \gamma\sin\varphi]w\,\mathrm{d}s - u_1 + u_3 + x_m - x_1 \tag{15}$$

$$F_n = \int_0^1 [(1+\varepsilon)\sin\varphi + \gamma\cos\varphi]w\,\mathrm{d}s + u_2 - u_4 + y_1 - y_m \tag{16}$$

where $[x_1 \;\; y_1]^T = \boldsymbol{r}(\boldsymbol{b}, 0)$ and $[x_m \;\; y_m]^T = \boldsymbol{r}(\boldsymbol{b}, 1)$ are the coordinates of both end nodes of the beam, $p_z = p_z(\boldsymbol{b}, s)$ are external distributed moments per unit length of the centroid curve, and $w = w(\boldsymbol{b}, s) = \|\boldsymbol{r}'\|$.

Note that the last two components of $\boldsymbol{F}$ are kinematic quantities rather than forces. Consequently, the matrix $\partial \boldsymbol{F}/\partial \boldsymbol{u}$ can not be regarded as a tangential stiffness matrix in the conventional sense. This fact, however, does not change anything in the usual finite element procedures because $\partial \boldsymbol{F}/\partial \boldsymbol{u}$ is still symmetric and nothing needs to be altered in the structural assemblage process. Furthermore, the considerations regarding the regularity of a conventional tangential stiffness matrix are also valid for the matrix $\partial \boldsymbol{F}/\partial \boldsymbol{u}$. On the other hand, in the eigenvalue problem formulation, we need the conventional stiffness matrix. For this purpose the internal DOF are eliminated numerically.

The nonzero derivatives of element internal forces, with respect to the element response variables, can be written as

$$\frac{\partial F_1}{\partial u_{n-1}} = -1, \qquad \frac{\partial F_2}{\partial u_n} = 1, \qquad \frac{\partial F_3}{\partial u_{n-1}} = 1, \qquad \frac{\partial F_4}{\partial u_n} = -1 \tag{17}$$

$$\frac{\partial F_{n-1}}{\partial u_1} = -1, \qquad \frac{\partial F_{n-1}}{\partial u_3} = 1, \qquad \frac{\partial F_n}{\partial u_2} = 1, \qquad \frac{\partial F_n}{\partial u_4} = -1 \tag{18}$$

and, for $5 \le j \le n$,

$$\frac{\partial F_{i+4}}{\partial u_j} = \int_0^1 \left(EI\frac{P_i'}{w}\frac{\partial \phi'}{\partial u_j} + \left\{ \frac{\partial \gamma}{\partial u_j}[AE\varepsilon - A_s G(1+\varepsilon)] + \frac{\partial \varepsilon}{\partial u_j}\gamma(AE - A_s G) \right\} w P_i \right) \mathrm{d}s, \qquad 1 \le i \le m \tag{19}$$

$$\frac{F_{n-1}}{\partial u_j} = -\int_0^1 \left[\frac{\partial \varepsilon}{\partial u_j}\cos\varphi - (1+\varepsilon)\frac{\partial \varphi}{\partial u_j}\sin\varphi - \frac{\partial \gamma}{\partial u_j}\sin\varphi - \gamma\frac{\partial \varphi}{\partial u_j}\cos\varphi \right] w\,\mathrm{d}s \tag{20}$$

$$\frac{F_n}{\partial u_j} = \int_0^1 \left[\frac{\partial \varepsilon}{\partial u_j}\sin\varphi + (1+\varepsilon)\frac{\partial \varphi}{\partial u_j}\cos\varphi + \frac{\partial \gamma}{\partial u_j}\cos\varphi - \gamma\frac{\partial \varphi}{\partial u_j}\sin\varphi \right] w\,\mathrm{d}s \tag{21}$$

where, for $5 \le j \le n-2$, it follows that

$$\frac{\partial \varphi}{\partial u_j} = P_{j-4}, \qquad \frac{\partial \phi'}{\partial u_j} = P'_{j-4}$$

$$\frac{\partial \varepsilon}{\partial u_j} = \frac{-\lambda_1 \sin\varphi - \lambda_2 \cos\varphi}{AE} \frac{\partial \varphi}{\partial u_j}$$

$$\frac{\partial \gamma}{\partial u_j} = \frac{-\lambda_1 \cos\varphi + \lambda_2 \sin\varphi}{A_s G} \frac{\partial \varphi}{\partial u_j} \tag{22}$$

$$\frac{\partial \varphi}{\partial u_{n-1}} = 0, \qquad \frac{\partial \phi'}{\partial u_{n-1}} = 0$$

$$\frac{\partial \varepsilon}{\partial u_{n-1}} = \frac{\cos\varphi}{AE}, \qquad \frac{\partial \gamma}{\partial u_{n-1}} = \frac{-\sin\varphi}{A_s G} \tag{23}$$

$$\frac{\partial \varphi}{\partial u_n} = 0, \qquad \frac{\partial \phi'}{\partial u_n} = 0$$

$$\frac{\partial \varepsilon}{\partial u_n} = \frac{-\sin\varphi}{AE}, \qquad \frac{\partial \gamma}{\partial u_n} = \frac{-\cos\varphi}{A_s G} \tag{24}$$

V. Eigenfrequency Response Analysis

The natural frequencies of the structure are obtained as a part of the solution of the eigenvalue problem (3). For this purpose, one needs the matrices $\boldsymbol{K}^s$ and $\boldsymbol{M}^s$. These matrices are assembled from the corresponding element matrices $\boldsymbol{K}$ and $\boldsymbol{M}$.

Mass Matrix

Unfortunately, it is not possible to derive a consistent mass matrix for the employed beam element. This fact is due to the specific formulation of the element where only the rotation field is approximated.[2,3] Therefore, the idea was to find some other mass matrix that would give good results when combined with the proposed element. Thus several mass matrix concepts[21–23] were studied, and the results of the calculated eigenvalues were compared to the analytical solutions. Finally, the choice was made for the matrix proposed by Stavrinidis et al.[23] In that work, the higher-order approach is used where it is assumed that the stiffness and mass matrices may be expanded in series as

$$[\boldsymbol{K}] = \lfloor \boldsymbol{K}_0 + \lambda^2 \boldsymbol{K}_4 + \cdots \rfloor, \qquad [\boldsymbol{M}] = \lfloor \boldsymbol{M}_0 + \lambda^2 \boldsymbol{M}_4 + \cdots \rfloor \tag{25}$$

By keeping only the first two terms, one obtains a quadratic eigenproblem of the form

$$\lfloor \boldsymbol{K}_0 - \lambda \boldsymbol{M}_0 - \lambda^2 (\boldsymbol{M}_2 - \boldsymbol{K}_4) \rfloor \varphi_q = 0 \tag{26}$$

When the first- and the second-order eigenvalue problems are compared, it is possible to derive a mass matrix for the first-order problem that contains the effects of the second-order parts. The details of this procedure are given in Ref. 23. Assuming a six-DOF beam element (two displacements and one rotation for each of both end nodes), the final form of the matrix is

$$\boldsymbol{M} = \frac{\rho A L}{420} \begin{bmatrix} 140 & 0 & 0 & 70 & 0 & 0 \\ 0 & 163 & 25.5L & 0 & 47 & -9.5L \\ 0 & 25.5L & 7.5L^2 & 0 & 9.5L & -3L^2 \\ 70 & 0 & 0 & 140 & 0 & 0 \\ 0 & 47 & 9.5L & 0 & 163 & -25.5L \\ 0 & -9.5L & -3L^2 & 0 & -25.5L & 7.5L^2 \end{bmatrix} \tag{27}$$

where $L = L(\boldsymbol{b})$ is the element length. Note that the mass per unit length ρA and the flexural rigidity EI are assumed to be constant along the beam. This is the reason for dropping in Eq. (4) the dependency of cross-sectional quantities on the parameter s of the element. Additionally, note that the preceding matrix was derived for a prismatic slender beam.

Stiffness Matrix

As already mentioned, the employed beam element has more DOF than it is assumed by the employed mass matrix. To be more precise, the element internal DOF need to be eliminated to make $\boldsymbol{K}$ and $\boldsymbol{M}$ a matching couple. Employing the usual matrix condensation technique, one can proceed as follows. When it is assumed that the inertial forces corresponding to internal DOF are negligible, the basic modal equation (without damping) can be written as

$$\begin{bmatrix} 0 & 0 \\ 0 & \boldsymbol{M} \end{bmatrix} \begin{bmatrix} \ddot{\boldsymbol{u}}^{\text{int}} \\ \ddot{\boldsymbol{u}}^{\text{ext}} \end{bmatrix} + \begin{bmatrix} \boldsymbol{K}^{ii} & \boldsymbol{K}^{ie} \\ \boldsymbol{K}^{ei} & \boldsymbol{K}^{ee} \end{bmatrix} \begin{bmatrix} u^{\text{int}} \\ u^{\text{ext}} \end{bmatrix} = \begin{bmatrix} 0 \\ 0 \end{bmatrix} \tag{28}$$

where $\boldsymbol{K}^{ii} = \partial \boldsymbol{F}^{\text{int}} / \partial \boldsymbol{u}^{\text{int}}$, $\boldsymbol{K}^{ie} = \partial \boldsymbol{F}^{\text{int}} / \partial \boldsymbol{u}^{\text{ext}}$, $\boldsymbol{K}^{ei} = \partial \boldsymbol{F}^{\text{ext}} / \partial \boldsymbol{u}^{\text{int}}$, and $\boldsymbol{K}^{ee} = \partial \boldsymbol{F}^{\text{ext}} / \partial \boldsymbol{u}^{\text{ext}}$. Here, the superscripts int and ext are quantities corresponding to internal and external DOF, respectively. By eliminating $\boldsymbol{u}^{\text{int}}$ from Eq. (28), one can derive

$$\boldsymbol{M} \ddot{\boldsymbol{u}}^{\text{ext}} + [\boldsymbol{K}^{ee} - \boldsymbol{K}^{ei} (\boldsymbol{K}^{ii})^{-1} \boldsymbol{K}^{ie}] \boldsymbol{u}^{\text{ext}} = 0 \tag{29}$$

wherefrom it follows that

$$\boldsymbol{K} = \boldsymbol{K}^{ee} - \boldsymbol{K}^{ei} (\boldsymbol{K}^{ii})^{-1} \boldsymbol{K}^{ie} \tag{30}$$

The inversion of the matrix $\boldsymbol{K}^{ii}$ has to be done numerically.

VI. Design Sensitivity Analysis

The design sensitivity analysis comprises the design derivatives calculation of both the static response variables $\mathrm{d}\boldsymbol{u}^s/\mathrm{d}\boldsymbol{b}$ and the eigenvalues $\mathrm{d}\lambda_1/\mathrm{d}\boldsymbol{b}$, $\mathrm{d}\lambda_2/\mathrm{d}\boldsymbol{b}$, ...

Design Derivatives of Static Response Variables

The common sensitivity equation

$$\frac{\mathrm{d}\boldsymbol{u}^s}{\mathrm{d}\boldsymbol{b}} = \left(\frac{\partial \boldsymbol{F}^s}{\partial \boldsymbol{u}^s} \right)^{-1} \left(\frac{\mathrm{d}\boldsymbol{R}^s}{\mathrm{d}\boldsymbol{b}} - \frac{\partial \boldsymbol{F}^s}{\partial \boldsymbol{b}} \right) \tag{31}$$

is derived by differentiating the response equation (2) with respect to $\boldsymbol{b}$ and rearranging the terms. Here, the matrix $(\partial \boldsymbol{F}^s/\partial \boldsymbol{u}^s)^{-1}$ is already known from the response analysis. The matrix $\mathrm{d}\boldsymbol{R}^s/\mathrm{d}\boldsymbol{b}$ is nonzero if the externally applied nodal loads are design dependent. However, because $\boldsymbol{R}$ is more precisely defined only in a specific design problem, no further instructions can be offered. Finally, the matrix $\partial \boldsymbol{F}^s/\partial \boldsymbol{b}$ is obtained by assembling the element matrices $\partial \boldsymbol{F}/\partial \boldsymbol{b}$. The nonzero elements of $\partial \boldsymbol{F}/\partial \boldsymbol{b}$ can be written as

$$\frac{\partial F_1}{\partial \boldsymbol{b}} = 0, \qquad \frac{\partial F_2}{\partial \boldsymbol{b}} = 0, \qquad \frac{\partial F_3}{\partial \boldsymbol{b}} = -\int_0^1 \left(\frac{\mathrm{d}p_x}{\mathrm{d}\boldsymbol{b}} w + p_x \frac{\mathrm{d}w}{\mathrm{d}\boldsymbol{b}} \right) \mathrm{d}s$$

$$\frac{\partial F_4}{\partial \boldsymbol{b}} = -\int_0^1 \left(\frac{\mathrm{d}p_y}{\mathrm{d}\boldsymbol{b}} w + p_y \frac{\mathrm{d}w}{\mathrm{d}\boldsymbol{b}} \right) \mathrm{d}s \tag{32}$$

$$\frac{\partial F_{i+4}}{\partial \boldsymbol{b}} = \int_0^1 \left[E \frac{P'_i}{w} \left(\frac{\mathrm{d}I}{\mathrm{d}\boldsymbol{b}} - \frac{I}{w} \frac{\mathrm{d}w}{\mathrm{d}\boldsymbol{b}} \right) \right] \mathrm{d}s + \int_0^1 \left\{ \frac{\mathrm{d}w}{\mathrm{d}\boldsymbol{b}} [AE\gamma\varepsilon - A_s G\gamma(1+\varepsilon) - p_z] + \frac{\mathrm{d}A}{\mathrm{d}\boldsymbol{b}} Ew\gamma\varepsilon - \frac{\mathrm{d}A_s}{\mathrm{d}\boldsymbol{b}} Gw\gamma(1+\varepsilon) - \frac{\mathrm{d}p_z}{\mathrm{d}\boldsymbol{b}} w + \frac{\partial \gamma_s}{\partial \boldsymbol{b}} [AEw\varepsilon - A_s Gw(1+\varepsilon)] + \frac{\partial \varepsilon}{\partial \boldsymbol{b}} [w\gamma(AE - A_s G)] \right\} P_i \, \mathrm{d}s, \qquad 1 \le i \le m \tag{33}$$

$$\frac{\partial F_{n-1}}{\partial \boldsymbol{b}} = -\int_0^1 [(1+\varepsilon)\cos\varphi - \gamma \sin\varphi] \frac{\mathrm{d}w}{\mathrm{d}\boldsymbol{b}} \mathrm{d}s - \int_0^1 \left(\frac{\partial \varepsilon}{\partial \boldsymbol{b}} \cos\varphi - (1+\varepsilon)\sin\varphi \frac{\partial \varphi}{\partial \boldsymbol{b}} - \frac{\partial \gamma}{\partial \boldsymbol{b}} \sin\varphi - \gamma \cos\varphi \frac{\partial \varphi}{\partial \boldsymbol{b}} \right) w \, \mathrm{d}s - \frac{\mathrm{d}x_m}{\mathrm{d}\boldsymbol{b}} - \frac{\mathrm{d}x_1}{\mathrm{d}\boldsymbol{b}} \tag{34}$$

$$\frac{\partial F_n}{\partial \boldsymbol{b}} = \int_0^1 [(1+\varepsilon)\sin\varphi + \gamma\cos\varphi]\frac{\mathrm{d}w}{\mathrm{d}\boldsymbol{b}}\mathrm{d}s + \int_0^1 \left(\frac{\partial\varepsilon}{\partial\boldsymbol{b}}\sin\varphi + (1+\varepsilon)\cos\varphi\frac{\partial\varphi}{\partial\boldsymbol{b}} + \frac{\partial\gamma}{\partial\boldsymbol{b}}\cos\varphi - \gamma\sin\varphi\frac{\partial\varphi}{\partial\boldsymbol{b}}\right)w\,\mathrm{d}s + \frac{\mathrm{d}y_1}{\mathrm{d}\boldsymbol{b}} - \frac{\mathrm{d}y_m}{\mathrm{d}\boldsymbol{b}} \tag{35}$$

where

$$\frac{\partial\varepsilon}{\partial\boldsymbol{b}} = -\frac{\lambda_1\cos\varphi - \lambda_2\sin\varphi}{EA^2}\frac{\mathrm{d}A}{\mathrm{d}\boldsymbol{b}} + \frac{1}{EA}\left(\frac{\partial\lambda_1}{\partial\boldsymbol{b}}\cos\varphi - \lambda_1\sin\varphi\frac{\partial\varphi}{\partial\boldsymbol{b}} - \frac{\partial\lambda_2}{\partial\boldsymbol{b}}\sin\varphi - \lambda_2\cos\varphi\frac{\partial\varphi}{\partial\boldsymbol{b}}\right) \tag{36}$$

$$\frac{\partial\gamma}{\partial\boldsymbol{b}} = \frac{\lambda_1\sin\varphi + \lambda_2\cos\varphi}{GA_s^2}\frac{\mathrm{d}A_s}{\mathrm{d}\boldsymbol{b}} + \frac{1}{GA_s}\left(-\frac{\partial\lambda_1}{\partial\boldsymbol{b}}\sin\varphi - \lambda_1\cos\varphi\frac{\partial\varphi}{\partial\boldsymbol{b}} - \frac{\partial\lambda_2}{\partial\boldsymbol{b}}\cos\varphi + \lambda_2\sin\varphi\frac{\partial\varphi}{\partial\boldsymbol{b}}\right) \tag{37}$$

$$\frac{\partial\lambda_1}{\partial\boldsymbol{b}} = -\int_0^s \left(\frac{\mathrm{d}p_x}{\mathrm{d}\boldsymbol{b}}w + p_x\frac{\mathrm{d}w}{\mathrm{d}\boldsymbol{b}}\right)\mathrm{d}q$$

$$\frac{\partial\lambda_2}{\partial\boldsymbol{b}} = \int_0^s \left(\frac{\mathrm{d}p_y}{\mathrm{d}\boldsymbol{b}}w + p_y\frac{\mathrm{d}w}{\mathrm{d}\boldsymbol{b}}\right)\mathrm{d}q \tag{38}$$

$$\frac{\partial\varphi}{\partial\boldsymbol{b}} = \frac{1}{x'^2+y'^2}\left(x'\frac{\mathrm{d}y'}{\mathrm{d}\boldsymbol{b}} - y'\frac{\mathrm{d}x'}{\mathrm{d}\boldsymbol{b}}\right)$$

$$\frac{\mathrm{d}w}{\mathrm{d}\boldsymbol{b}} = \frac{1}{\sqrt{x'^2+y'^2}}\left(x'\frac{\mathrm{d}x'}{\mathrm{d}\boldsymbol{b}} + y'\frac{\mathrm{d}y'}{\mathrm{d}\boldsymbol{b}}\right), \qquad [x \quad y]^T = \hat{\boldsymbol{r}}(\boldsymbol{b}, s) \tag{39}$$

Design Derivatives of Eigenfrequencies

When it is assumed that all structural eigenfrequencies are single (nonrepetead), the design derivatives may be obtained as follows.[24] By taking the design derivative of the eigenvalue equation (3), one obtains

$$\frac{\partial\boldsymbol{K}^s}{\partial\boldsymbol{b}}\boldsymbol{\varphi}_j + \boldsymbol{K}^s\frac{\partial\boldsymbol{\varphi}_j}{\partial\boldsymbol{b}} = \frac{\partial\lambda}{\partial\boldsymbol{b}}\boldsymbol{M}^s\boldsymbol{\varphi}_j + \lambda_j\frac{\partial\boldsymbol{M}^s}{\partial\boldsymbol{b}}\boldsymbol{\varphi}_j + \lambda\boldsymbol{M}^s\frac{\partial\boldsymbol{\varphi}_j}{\partial\boldsymbol{b}} \tag{40}$$

If the symmetry of the mass matrix is considered and the eigenvectors are normalized with respect to the mass matrix, the eigenvalue derivative may be expressed from Eq. (40) as

$$\frac{\partial\lambda_j}{\partial\boldsymbol{b}} = \boldsymbol{\varphi}_j^T\left(\frac{\partial\boldsymbol{K}^s}{\partial\boldsymbol{b}} - \lambda_j\frac{\partial\boldsymbol{M}^s}{\partial\boldsymbol{b}}\right)\boldsymbol{\varphi}_j \tag{41}$$

where the matrices $\partial\boldsymbol{M}^s/\partial b_i, i = 1, \ldots, N_b$, are assembled from corresponding element matrices $\partial\boldsymbol{M}/\partial b_i$ that can be calculated straightforwardly. Similarly, the matrices $\partial\boldsymbol{K}^s/\partial b_i$, $i = 1, \ldots, N_b$, are assembled from corresponding element matrices

$$\frac{\partial\boldsymbol{K}}{\partial\boldsymbol{b}_i} = \frac{\partial[\boldsymbol{K}^{ee} - \boldsymbol{K}^{ei}(\boldsymbol{K}^{ii})^{-1}\boldsymbol{K}^{ie}]}{\partial b_i} \tag{42}$$

To calculate these matrices, one needs the element matrices $\partial^2\boldsymbol{F}/\partial\boldsymbol{u}^s\partial\boldsymbol{b}_i$. These can be expressed analytically by differentiating Eqs. (17–21). The expressions for the particular design derivatives are very expansive, and for this reason they are not presented here. They are listed in Ref. 25.

VII. Examples

To illustrate the theory, two minimal volume design problems will be considered. A 6-node beam element with 10 Gauss integration points and the described[23] mass matrix formulation are used in both examples. Both design problems have been solved by employing the subroutine AMOPT.[17]

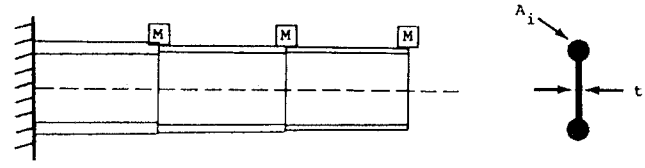

Fig. 3 Cantilevered beam.

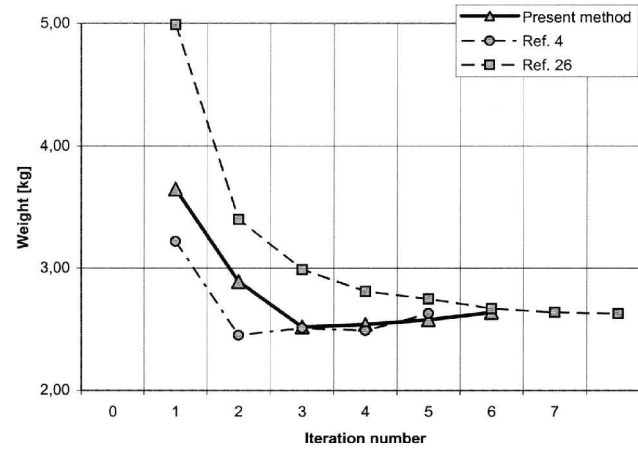

Fig. 4 Iteration history.

Cantilever Beam Cross-Section Optimization

This example represents a rather conventional design problem already considered in Refs. 4 and 26. Here, this problem is addressed to compare the results of the proposed approach with the results given in cited references. For the sake of clarity, the original units used in the references are written in parentheses.

The cantilever beam considered is shown in Fig. 3. The length of each section is 0.508 m (20 in.), and the depth is 0.1524 m (6 in.). The beam is symmetric about the midplane and supports three nonstructural masses of 13.608 kg (30 lb) each. Young's modulus is $E = 71020$ MPa (10.3×10^6 psi), Poisson's ratio is 0.3, and the density is $\rho = 2768\ \mathrm{kg}\cdot\mathrm{m}^{-3}$ (0.1 pci).

The design variables are the flange areas A_1, A_2, and A_3 and the web thickness t_1, t_2, and t_3. The initial design is $b_{1,2,3} = A_{1,2,3} = 6.453 \times 10^4\ \mathrm{m}^2$ (1.0 in.^{2}) and $b_{4,5,6} = t_{1,2,3} = 2.54 \times 10^{-3}$ m (0.1 in.). Lower bounds are $A^{\mathrm{low}}_{1,2,3} = 6.452 \times 10^{-6}$ m^2 (0.01 in.^{2}) and $t^{\mathrm{low}}_{1,2,3} = 2.54 \times 10^{-5}$ m (0.001 in.).

The design problem is formulated as follows: Find such values of the design variables that, while minimizing the volume of the structure, the fundamental frequency will not be smaller than $f^{\mathrm{low}} = 20$ Hz.

Mathematically this can be written as

$$\min\ \rho\sum_{i=1}^{3}\left(\int_0^1 A_i(\boldsymbol{b})\|\boldsymbol{r}_i'(t)\|\,\mathrm{d}t\right) \tag{43}$$

subject to constraints

$$f(\boldsymbol{b}, {}^s\boldsymbol{u}) - f^{\mathrm{low}} \le 0, \qquad b_1, b_2, b_3 \ge 6.452E-6$$
$$b_4, b_5, b_6 \ge 2.54E-5 \tag{44}$$

As can be seen from the iteration history in Fig. 4, a near-optimum design is reached in the sixth iteration. The optimization results are listed in Table 1, together with the cited ones.

The optimal weight (objective function value) is equal to that from Refs. 4 and 26. One can conclude that the presented method was in this case more efficient than the approach of Ref. 26 and comparable to the approach of Ref. 4.

Shape Optimization of a Simple Bridge Structure

The second example concerns a shape design problem of a simple eight-element bridge structure shown in Fig. 5. The problem

Table 1 Optimization results for the cantilever beam

Parameter	Value	Ref. 4	Ref. 26
Weight, kg	2.63	2.63	2.63
Frequency, Hz	20.00	20.00	20.00
A_1, m^2	$5.39E{-}04$	$5.37E{-}04$	$5.30E{-}04$
A_2, m^2	$2.97E{-}04$	$2.93E{-}04$	$2.98E{-}04$
A_3, m^2	$9.73E{-}05$	$9.74E{-}05$	$8.71E{-}05$
t_1, m	$2.64E{-}05$	$2.54E{-}05$	$1.52E{-}04$
t_2, m	$2.64E{-}05$	$2.54E{-}05$	$1.52E{-}04$
t_3, m	$2.64E{-}05$	$2.54E{-}05$	$1.27E{-}04$

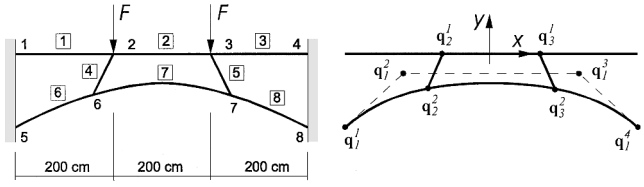

Fig. 5 Simple bridge structure.

was already considered in Ref. 16, where only the nodal displacements were constrained. Here, the same problem is extended by adding it the fundamental frequency constraint. The fundamental frequency corresponding to the starting design in Ref. 16 is 13.42 rad/s, whereas at the optimum design it is 12.32 rad/s. In the present example, the fundamental frequency is limited to 14 rad/s to make sure that the frequency constraint will be active at the optimum.

The material data of the structure are as follows: $E = 210{,}000$ MPa and $G = 81{,}000$ MPa. The cross-sectional quantities for all elements are constant: $A = 20$ cm^2, $A_s = 4$cm^2, and $I = 350$ cm^4. At nodes 2 and 3, the structure is loaded in the vertical direction with $F = 500{,}000$ N.

The position and the shape of elements 1, 2, and 3 are not design dependent and are kept fixed during the design process. The rest of the structure, however, depends on four design variables b_j, $1 \le j \le 4$. These design variables influence the position and the shape of the first three design elements (DE). DE1 consists of beams 6–8; DE2 of beam 4; DE3 of beam 5; and DE4 of beams 1–3.

The design variables b_1 and b_3 influence the horizontal and the vertical positions of the control points $\boldsymbol{q}_1^2$ and $\boldsymbol{q}_1^3$. The design variable b_2 influences the vertical position of the control points $\boldsymbol{q}_1^1$ and $\boldsymbol{q}_1^4$ whereas b_4 influences the position of the nodes 6 and 7 along DE1.

The shape of DE1 is defined by

$$\boldsymbol{r}_1 = \sum_{j=1}^{4} B_{4,j}(t)\boldsymbol{q}_1^j, \qquad \boldsymbol{q}_1^1 = [-300 - b_2]^T$$

$$\boldsymbol{q}_1^2 = [-b_1 - b_3]^T, \qquad \boldsymbol{q}_1^3 = [b_1 - b_3]^T$$

$$\boldsymbol{q}_1^4 = [300 - b_2]^T \tag{45}$$

and the shapes of DE2 and DE3 by

$$\boldsymbol{r}_2 = \sum_{j=1}^{2} B_{2,j}(t)\boldsymbol{q}_2^j, \qquad \boldsymbol{r}_3 = \sum_{j=1}^{2} B_{2,j}(t)\boldsymbol{q}_3^j$$

$$\boldsymbol{q}_2^1 = [-100 \quad 0]^T, \qquad \boldsymbol{q}_2^2 = \hat{\boldsymbol{r}}_1\left(\boldsymbol{b}, c_1^2\right), \qquad \boldsymbol{q}_3^1 = [100 \quad 0]^T$$

$$q_3^2 = \hat{\boldsymbol{r}}_1\left(\boldsymbol{b}, c_1^3\right), \qquad c_1^2 = 0.5 - b_4, \qquad c_1^3 = 0.5 + b_4 \tag{46}$$

where $B_{ij}(t)$ is the Bernstein polynomial (see Ref. 27) and $t \in [0, 1]$. The shape of DE4 does not depend on $\boldsymbol{b}$ and is given by

$$\boldsymbol{r}_4 = [(600t - 300) \quad 0]^T \tag{47}$$

Now we can define the design problem as follows: Find such values of the design variables $0 \le b_1, b_2, b_3 \le 300$, and $0 \le b_4 \le 0.5$, so that, while minimizing the volume of the structure, vertical displacements v_2 and v_3 of the nodes 2 and 3, respectively, will not be greater than $v^{\text{upp}} = 5$ cm and the fundamental frequency will not be smaller than $f^{\text{low}} = 14$ rad/s. We can write

$$\min A \sum_{i=}^{4} \left(\int_0 \|\boldsymbol{r}_i'(\boldsymbol{b}, t)\| \, \mathrm{d}t \right) \tag{48}$$

subject to constraints

$$v_2(\boldsymbol{b}, {}^s\boldsymbol{u}) - v^{\text{upp}} \le 0, \qquad v_3(\boldsymbol{b}, {}^s\boldsymbol{u}) - v^{\text{upp}} \le 0$$

$$f(\boldsymbol{b}, {}^s\boldsymbol{u}) - f^{\text{low}} \le 0, \qquad 0 \le b_1, b_2, b_3 \le 300$$

$$0 \le b_4 \le 0.5 \tag{49}$$

The optimization results are given in Table 2. Compared to the initial structure, the optimized one exhibits a reduced volume by 7%, reduced vertical displacements by 16% at nodes 2 and 3, and the first natural frequency increased for 4.3%. Figure 6 shows all three structures.

The objective function (total volume) values, the first natural frequency and the design variables for all the iterations are listed in Table 3.

The example illustrates the principle of the proposed shape optimization technique and its efficacy. The optimum design is reached in only seven iterations.

Table 2 Bridge design problem-results

Parameter	Initial	Optimized; Ref. 16	Optimized with constrained frequency
b_1	200.00	76.24	141.80
b_2	100.00	86.24	77.86
b_3	50.00	0.00	0.00
b_4	0.2500	0.1954	0.2010
v_2, v_3	5.891	5.000	5.000
Fundamental frequency, rad/s	13.42	12.32	14.00
Volume, cm^3	28,408	25,685	26,019

Table 3 Iteration history

Iteration	Volume, cm^3	Frequency, rad/s	b_1	b_2	b_3	b_4
0	28408.00	13.42	200.000	100.000	50.000	0.250
1	27628.00	14.58	195.400	81.780	21.400	0.241
2	26295.00	14.40	166.700	90.250	0.827	0.193
3	25973.00	13.83	138.200	66.840	0.000	0.209
4	25988.00	13.87	149.900	82.050	0.099	0.192
5	25994.00	13.94	139.400	76.880	0.000	0.201
6	26009.00	13.91	140.700	77.900	0.379	0.201
7	26019.00	14.00	141.800	77.860	0.000	0.201

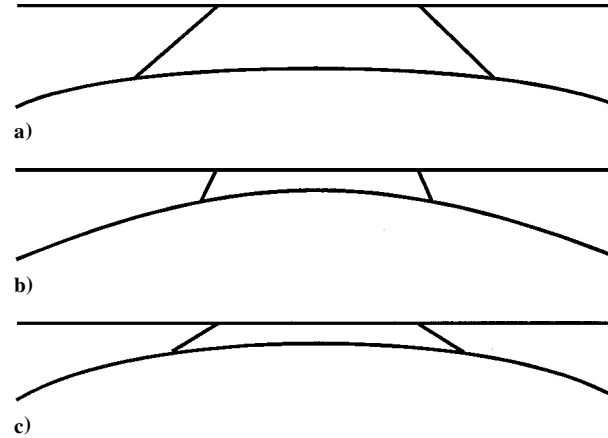

Fig. 6 Structures: a) initial shape, b) optimized without constrained frequency,[16] and c) optimized with constrained frequency.

VIII. Summary

An approach to shape optimal design of elastic planar frames with frequency constraints was proposed. A kinematically nonlinear beam element was employed that can handle almost arbitrary large displacements and rotations. The design element technique also proved to be a high-quality shape representation concept when frequency constraints are imposed on the structure. The definition of the design element by using a Bézier curve is very convenient because it considerably reduces the number of necessary design variables.

The inertial forces representationby the mass matrix, chosen from the literature, proved to give very accurate results for the natural frequencies when combined with the stiffness matrix of the employed beam element. Because analytical formulas for the design derivatives may be derived, the design sensitivity analysis is very efficient.

The numerical examples show that the optimization process itself is comparable to the previously proposed approaches. However, the presented approach can cover a wider scope of engineering problems.

References

[1]Prathap, G., "Field-Consistency—Toward a Science of Constrained Multi-Strain Field Finite Element Formulations," *SADHANA*, Vol. 9, 1986, pp. 319–344.

[2]Saje, M., "A Variational Principle for Finite Planar Deformation of Straight Slender Elastic Beams," *International Journal of Solids and Structures*, Vol. 26, No. 8, 1990, pp. 887–900.

[3]Saje, M., "Finite Element Formulation of Finite Planar Deformation of Curved Elastic Beams," *Computers and Structures*, Vol. 39, No. 3–4, 1991, pp. 327–337.

[4]Vanderplaats, G. N., and Salajegheh, E., "An Efficient Approximation Technique for Frequency Constraints in Frame Optimization," *International Journal for Numerical Methods in Engineering*, Vol. 26, No. 5, 1988, pp. 1057–1069.

[5]Wu, C. C., and Arora, J. S., "Design Sensitivity Analysis and Optimization of Nonlinear Structural Response Using Incremental Procedure," *AIAA Journal*, Vol. 25, No. 8, 1986, pp. 1118–1125.

[6]Khan, M. R., and Willmert, K. D., "An Efficient Optimality Criterion Method for Natural Frequency Constrained Structures," *Computers and Structures*, Vol. 14, No. 5–6, 1981, pp. 501–507.

[7]Ohno, T., Kramer, G. J. E., and Grierson, D. E., "Least-Weight Design of Frameworks Under Multiple Dynamic Loads," *Structural Optimization*, Vol. 1, No. 4, 1989, pp. 181–191.

[8]McGee, O. G., and Phan, K. F., "On the Convergence Quality of Minimum-Weight Design of Large Space Frames Under Multiple Dynamic Constraints," *Structural Optimization*, Vol. 4, No. 3–4, 1992, pp. 156–171.

[9]Chan, C. M., "An Optimality Criteria Algorithm for Tall Steel Building Design Using Commercial Standard Sections," *Structural Optimization*, Vol. 5, No. 1–2, 1992, pp. 26–29.

[10]Sadek, E. A., "Dynamic Optimization of Framed Structures with Variable Layout," *International Journal for Numerical Methods in Engineering*, Vol. 23, No. 7, 1986, pp. 1273–1294.

[11]Garstecki, A., and Therman, K., "Sensitivity of Frames to Variation of Hinges in Dynamic and Stability Problems," *Structural Optimization*, Vol. 4, No. 2, 1992, pp. 108–114.

[12]Kirsch, U., "Efficient Reanalysis for Topological Optimization," *Structural Optimization*, Vol. 6, No. 3, 1993, pp. 143–150.

[13]Wang, C. M., Ang, K. K., and Wang, L., "Optimization of Bracing and Internal Support Locations for Beams Against Lateral Buckling," *Structural Optimization*, Vol. 9, No. 1, 1995, pp. 12–17.

[14]Lepik, Ü., "Optimal Design of Elastic–Plastic Beams with Additional Supports," *Structural Optimization*, Vol. 9, No. 1, 1995, pp. 18–24.

[15]Grierson, D. E., and Pak, W. H., "Optimal Sizing, Geometrical and Topological Design Using a Genetic Algorithm," *Structural Optimization*, Vol. 6, No. 3, 1993, pp. 151–159.

[16]Kegl, M., Butinar, B. J., and Oblak, M. M., "Shape Optimal Design of Elastic Planar Frames with Non-linear Response," *International Journal for Numerical Methods in Engineering*, Vol. 38, No. 19, 1995, pp. 3227–3242.

[17]Kegl, M. S., Butinar, B. J., and Oblak, M. M., "Optimization of Mechanical Systems: On Strategy of Non-linear First-Order Approximation," *International Journal for Numerical Methods in Engineering*, Vol. 33, No. 2, 1992, pp. 223–234.

[18]Kegl, M., and Oblak, M. M., "Optimization of Mechanical Systems: On Non-linear First-Order Approximation with an Additive Convex Term," *Communications in Numerical Methods in Engineering*, Vol. 13, No. 1, 1997, pp. 13–20.

[19]Oblak, M. M. , Kegl, M., and Dinevski, D., "Shape Optimal Design of Elastic Planar Frames with Elastic and Skew-Sliding Supports," Design Engineering Technical Conf., American Society of Mechanical Engineers, Paper DETC97/DAC-3733, Sept. 1998.

[20]Rogers, D. F., and Adams, J. A., *Mathematical Elements for Computer Graphics*, McGraw–Hill, New York, 1990, pp. 289–304.

[21]Dawe, D. J., *Matrix and Finite Element Displacement Analysis of Structures*, Oxford Univ. Press, New York, 1984.

[22]Kim, K.-O., "A Review of Mass Matrices for Eigenproblems," *Computers and Structures*, Vol. 46, No. 6, 1993, pp. 1041–1048.

[23]Stavrinidis, C., Clinckemaille, J., and Dubois, J., "New Concepts for Finite-Element Mass Matrix Formulations," *AIAA Journal*, Vol. 27, No. 9, 1989, pp. 1249–1255.

[24]Nelson, R. B., "Simplified Calculation of Eigenvector Derivatives," *AIAA Journal*, Vol. 13, No. 9, 1976, pp. 1201–1205.

[25]Dinevski, D., "Optimiranje Oblike Dinamično Obremenjenih Linijskih Konstrukcij," Ph.D. Dissertation, Faculty of Mechanical Engineering, Univ. of Maribor, Maribor, Slovenia, 1997 (in Slovene).

[26]Woo, T. H., "Space Frame Optimization Subject to Frequency Constraints," *Proceedings of the 27th AIAA/ASME/ASCE/AHS Structures, Structural Dynamics, and Materials Conference*, AIAA, Reston, VA, 1986, pp. 103–115.

[27]Farin, G., *Curves and Surfaces for Computer Aided Geometric Design*, 2nd ed., Academic Press, New York, 1990, pp. 329–335.

E. R. Johnson
Associate Editor